International Journal of Computing Academic Research (IJCAR)
ISSN 2305-9184, Volume 5, Number 3 (June 2016), pp.163-169

http://www.meacse.org/ijcar

Use of an Effective Attenuation Coefficient Value and Material Filter Technique for Scatter Correction in Tc-99m SPECT

Inayatullah Shah Sayed and Siti Zubaidah Muda

Department of Diagnostic Imaging and Radiotherapy, Kulliyyah (Faculty) of Allied Health Sciences, International Islamic University Malaysia, Kuantan Campus, 25200 Kuantan, Pahang, Malaysia

Abstract

Accuracy in the diagnosis of disease in Tc-99m Single Photon Emission Computed Tomography is reduced due to the presence of scattered gamma photons in the image data. A range of scatter correction techniques exist, however, none is considered as the standard. The objective of this study is to apply a flat sheet of Aluminum 0.3mm thick as an absorber for the removal of scattered gamma photons and compare the image quality with those images obtained by using effective attenuation coefficient value. Data were acquired with the gamma camera (Philip ADAC Forte dual head) installed with LEHR collimator. A cylindrical phantom with cold and hot regions insert was scanned. Tc-99m radioactive material was introduced into the phantom. Images were reconstructed by using filtered back projection method. Perceived image quality and contrast of cold and hot regions, whereas, count profile and standard deviation in the count density of uniform region was measured. Quantitative analysis of all image quality parameters investigated show fair improvement with material filter. In conclusion, 0.3mm thickness of aluminum material filter may have some advantage over the use of effective attenuation coefficient value for scatter compensation when applied by scanning other ECT phantoms using Tc-99m radionuclide.

Keywords: SPECT, Scatter correction, contrast enhancement, material filter technique.

Introduction

Single Photon Emission Computed Tomography (SPECT) is commonly applied as a vital tool to provide functional and anatomical information of the organ under investigations in clinical studies. Gamma emitting radioactive material e.g. Tc-99m tagged with a suitable chemical compound is injected into the patient's body. Thus, SPECT inherits the issue of scattered gamma photons along with the others. Degradation of image quality is caused by the presence of scattered gamma photons. Presence of scatter in the image data is due the poor energy resolution of NaI(Tl) scintillator which is most commonly used for gamma photon detection. As a result nearly in all of the patient examinations 30 – 40% of recorded photons within the 20% energy window over the photopeak data are scattered gamma photons [1].

For the correction of scatter in SPECT, a number of researchers have developed a variety of techniques. These scatter compensation techniques are; use of asymmetric energy window over the photopeak to limit the scatter counts [2]. Use of the effective attenuation coefficient value 0.12/cm as an alternative of 0.15/cm value for 140 keV photons in water/tissue [3] when compensating the data for attenuation. There is another type of scatter correction technique, which uses material filter for removal of scatter before they are detected [4-7]. It was reported that material filter reduce the scattered gamma photons which are low energy relative to un-scattered photons from reaching the surface of detector of the system before their detection. However, there are some problems relevant to the softness and fragility of material (tin), as well as the thickness that was used. On the other hand, with the use of effective attenuation coefficient value the image data is either over or under corrected. Therefore, in the present study, Aluminum 0.3mm material filter has been applied,

which is stiffer than the tin (Sn) and as well cost effective. It is expected that, the material filter may provide good results in terms of image quality.

Materials and Methods

SPECT data acquisition and image reconstruction

Philip ADAC Forte imaging system installed with LEHR collimator was used. An insert with cold and hot regions placed into the cylindrical tank was scanned [8]. It is comprised of eight pairs of each, i.e., cold regions in hot background and hot regions in cold background of various sizes (4.7, 5.9, 7.3, 9.2, 11.4, 14.3, 17.9 and 22.4 mm) in 'V' shape. Cold and hot region parts were aligned for achieving similar cross sectional views to measure and compare the performance of radionuclide imaging systems. 20 mCi of Tc-99m radioactivity was distributed homogenously in the phantom. A flat sheet of aluminum material sized 56cm x 46cm and thickness of 0.30mm was used based on calculations of percent attenuation of a range of gamma photon energies by various thicknesses of Al material [9]. The image data were collected within a ±10% energy window centered at 140keV. The matrix size 128x128x16 was selected. Ninety (90) views were taken over 360^{o} (20 seconds / view). First, data were acquired without material filter, then; filter was mounted on the outer surface of collimator maintaining the same position of the phantom. Moreover, data acquisition parameters remained same for without and with filter.

Filtered back projection image reconstruction technique was used to reconstruct images from the data acquired without and with material filter. Mathematical filter i.e., Butterworth filter was selected with a cut-off frequency of 0.35 cycles/cm and order 5. Butterworth filter functions (cut-off frequency and order) value was chosen because of the frequent use in the department. Chang's attenuation correction technique with linear attenuation coefficient (LAC) values 0.12 cm^{-1} (without material filter) and 0.13 cm^{-1} (with material filter) was incorporated in the image reconstruction process. In addition, prior to image reconstruction both data sets were amended for the centre of rotation (COR), uniformity and decay correction. Furthermore, all images were saved in jpeg format for further analysis using the ImageJ software [10].

Images were analyzed in terms of count profile of uniform, cold and hot regions. The cold and hot regions contrast and standard deviation (SD) in the counts of uniform region were measured by using equation 1, 2 and 3, respectively.

$$C_{\text{cold region}} = \frac{D_{reg} - D_{bkg}}{D_{bkg}} \quad (1)$$

where D_{reg} is the average counts in cold region, and D_{bkg} is the average counts in the background.

$$C_{\text{hot region}} = \frac{D_{reg} - D_{bkg}}{D_{reg} + D_{bkg}} \quad (2)$$

where D_{reg} is the average counts in hot region and D_{bkg} is the average counts in the background.

$$SD = \sqrt{\frac{\sum_{i=1}^{N}(Z_i - D_{mean})^2}{(N-1)}} \quad (3)$$

where Z_i refers as the number of counts in the i^{th} pixel and N is the total number of pixels in region of interest (ROI). The D_{mean} refers to the mean count density/pixel under the ROI.

Images reconstructed from the data, i.e., use of effective attenuation coefficient value (without) and with material filter were compared in terms of visual, count profile, contrast and SD analysis. Also cold and hot regions detectability was investigated.

Results and Discussion

Over and under correction of the SPECT data for scatter causes difficulties in diagnosis of diseases. Diagnostic accuracy of any abnormality largely depends upon the quality of the clinical image. Improved quality images facilitate the specialist to make correct decision about the health condition of the patient. Hence, the best possible care of the patient can be made. This research was undertaken to investigate the result of using a material filter (aluminum 0.3 mm thick) into the improvement of SPECT image quality by removing some fraction of scattered events from the raw acquired data.

Visual, count profile and standard deviation analysis of uniform region images

For visual, count profile and standard deviation in the average count density of the uniform region analysis, same slice number of uniform region image (in each case) i.e., without material filter (effective attenuation coefficient value, $0.12/cm^{-1}$) and with material filter was selected. Images are shown in Fig. 1(a) without material filter and Fig. 1(b) with material filter. Without material filter image show the uniform distribution of radioactivity throughout the region. In contrast, material filtered image depicts inhomogeneous concentration of the radioactive material in the encircled part (Fig. 1b).

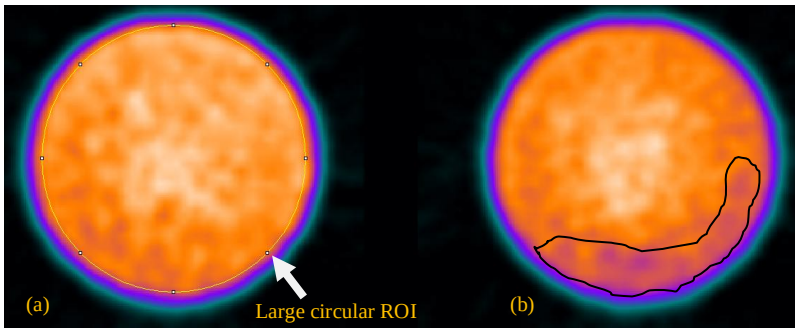

Fig. 1 (a) and (b) Show the uniform region image (a) without material filter and (b) with material filter.

Count profile was obtained by drawing a straight line through the centre of both of the regions, as shown in Fig. 2 (a) and (b). In the centre of count profile of both images gray scale value (count density) shows a higher value relative to the sides of both uniform region images. However, with material filter, count density in the periphery of the phantom indicates the uniform concentration of the radioactivity compared to the image obtained by using the effective attenuation coefficient value (without material filter).

Standard deviation in the uniform region without material filter and with material filter was found as 21.81 and 20.35, respectively. Thus, there is 7% reduction in the SD with material filter, which reflects that the material filter has reduced the noise from image by absorbing some fraction of scattered gamma photons which are considered as a noise component in SPECT images.

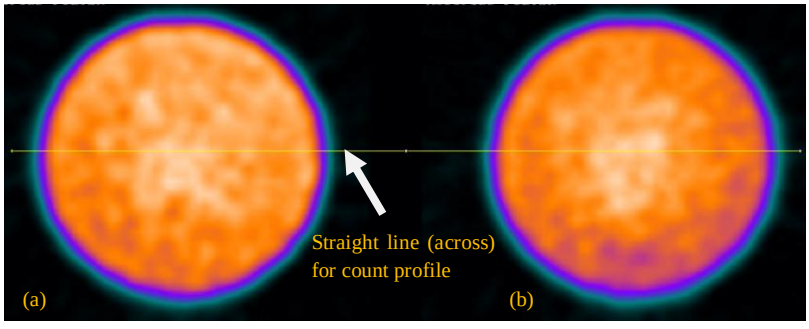

Fig. 2 (a) and (b) Show the straight line drawn across the centre of both images for plotting the count profile.

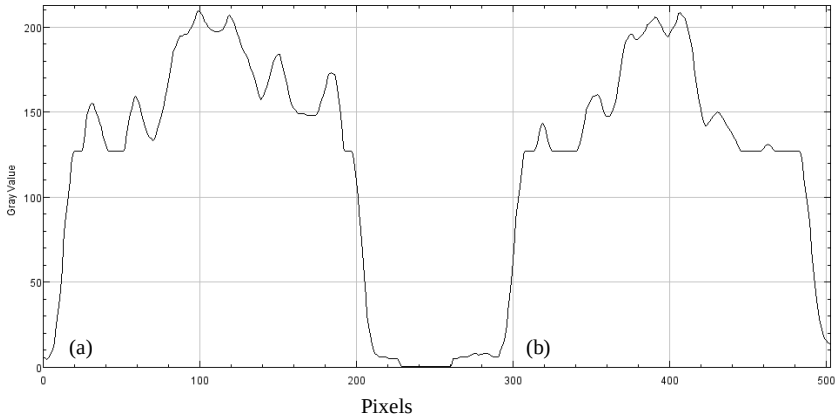

Fig. 3 (a) and (b) Count profiles taken through the centre of uniform region images (a) without material filter and (b) with material filter.

Cold region image analysis

Perceived image quality analysis of cold regions image (Fig. 4 b) with material filter represent that the larger cold region pair (22.4mm) pointed by the white arrow shows less count density in the centre of the cold region compared to the image shown in Fig. 4a (without material filter). This is the indication of the removal of some fraction of scattered gamma photons by material filter. In principle, there should be no radioactivity in the cold spot. Furthermore, uniform background can be observed in the image produced from material filtered data. Relating to the other cold spots, it is difficult to notice the difference between the images of two different data sets.

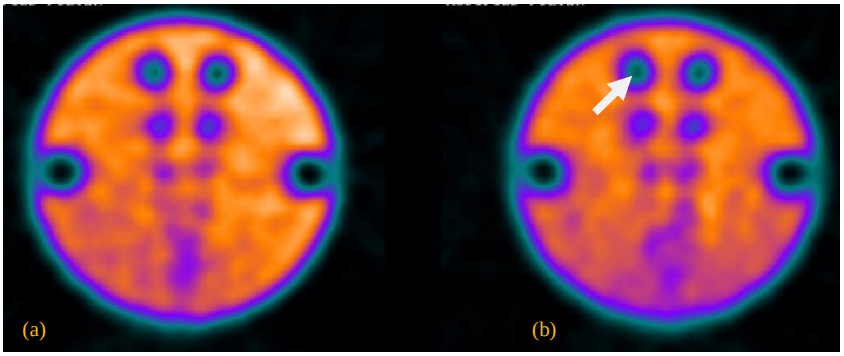

Fig. 4 (a) and (b) Cold region images (a) without material filter and (b) with material filter.

Quantitative analysis of cold regions was done by measuring the contrast using Eq. 1 as it is one of the parameter to investigate in terms of image quality. It can be seen in Fig. 5 that there is 9% increase in the measured contrast of cold region sized (22.4 mm diameter) with material filter compared to effective attenuation value (without material filter). However, in the case of small size cold regions, i.e., 17.9 mm and 14.3 mm diameter, contrast with material filter is degraded. In this analysis remaining small cold regions were excluded because of their un-sharp boundaries and un-detectability. Thus it was difficult to set the ROI inside the region. Also only single cold spot of the pair was considered due to the similar size as well as the position in the phantom.

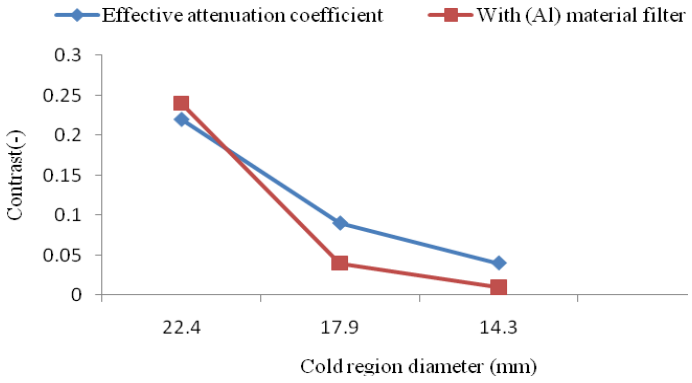

Fig. 5 Measured contrast of cold regions obtained from the data of using effective attenuation coefficient (without material filter) and with material filter.

In the count profile analysis only two cold regions (numbered as 1 and 2) can be seen, remaining cold regions are not detectable. In Fig. 6(b) it is clearly noticed that the filter has removed scattered gamma photons from the centre of the region, which has been already observed in terms of contrast value of that particular cold region.

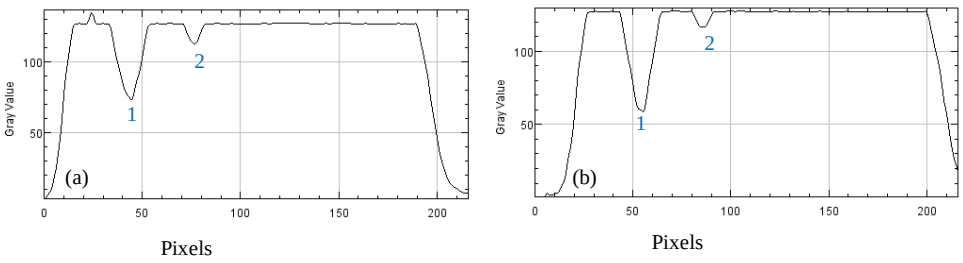

Fig. 6 Count profiles plotted by drawing the line crossing the centers of all cold regions (a) effective attenuation coefficient (without material filter) and (b) with material filter.

Hot region image analysis

From the visual inspection of hot region images shown in Fig. 7 (a) and (b), there is no change in the detectability of hot regions either without or with material filter. Thus, particularly, in this study it can be assumed that the material filter is not effective as compared to cold region images. It is well accepted that cold regions are more affected by the scattered gamma photons relative to hot regions.

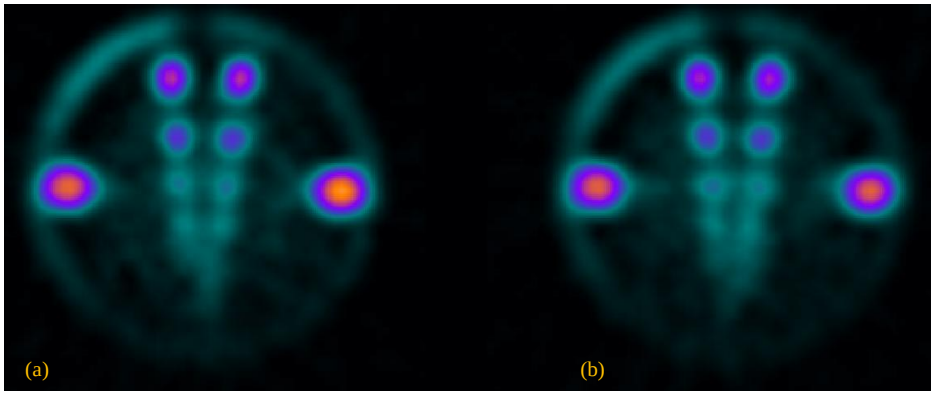

Fig. 7 (a) and (b) Hot region images (a) without material filter and (b) with material filter.

Hot region contrast was measured by using Eq. 2. With material filter, a marginal loss in the contrast is recorded as compared to the use of effective attenuation coefficient value, shown in Fig. 8. The difference is only about 2 – 3% which can be considered negligible. In other words there is no loss or gain with the use of Aluminum (0.3mm thick) material filter.

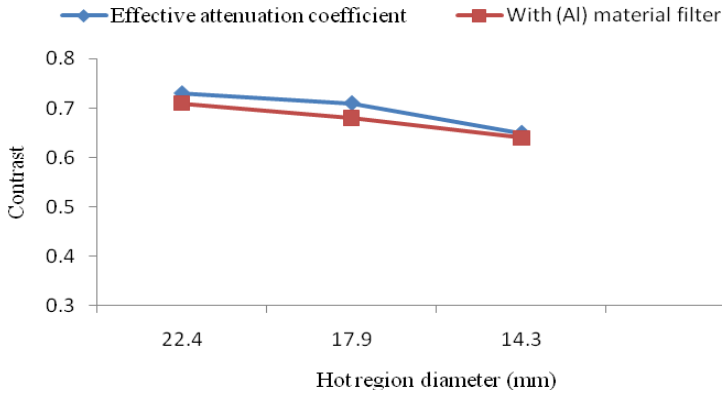

Fig. 8 Measured contrast of hot regions obtained from the data of using effective attenuation coefficient (without material filter) and with material filter.

Count profiles of hot regions were plotted similarly as for cold regions, Fig 9(a) and (b). Hot region image count profile (Fig. 9b) shows that the scattered gamma photons are removed by a material filter from the space between hot region of 2nd and 3rd pair, represented by a circle in red color (Fig 9b). Moreover, an additional small peak of 5th hot region is visible marked with a circle in blue color.

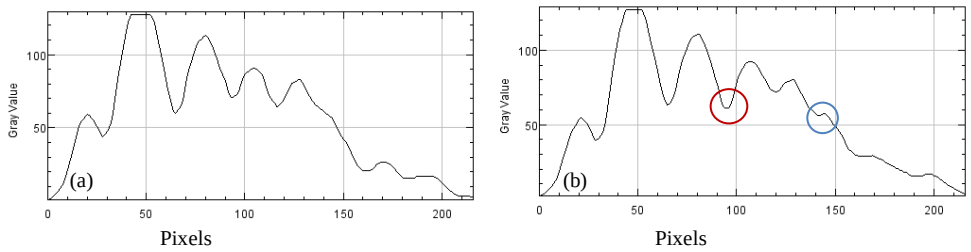

Fig. 9 Count profiles plotted by drawing the line crossing the centers of all hot regions (a) effective attenuation coefficient (without material filter) and (b) with material filter.

Visual analysis of the data does not reflect the improvement with material filter in the parameters investigated. However, quantitative analysis of uniform region images, such as; count profile, standard deviation in the count density of uniform images, contrast of cold regions and count profile analysis of both types of regions show some improvement with the use of material filter.

Conclusion

Quantitative analyses of results suggest that, in general the material filter technique improved the overall image quality compared to the use of effective attenuation coefficient value for scatter compensation. Thus, for further investigations Aluminum material filter with lower thickness (small value) may be applied for more complicated ECT phantoms, in order to find the applicability of the technique in clinical studies.

Acknowledgement

The authors are thankful to the Department of Nuclear Medicine, Radiotherapy and Oncology, Universiti Sains Malaysia for providing facilities to carry out experimental work for this study.

References

[1] B. F. Hutton, I. Buvat, and F. J. Beekman, "Review and current status of SPECT scatter correction," Phys. Med. Biol., vol. 56, pp. R85- R112, 2011.
[2] I. Buvat, H. Benali, A. Todd-Pokropek, and R. Di Paola, "A new correction method for gamma camera nonuniformity due to energy response variability," Phys. Med. Biol., vol. 40, pp. 1357-1374, 1995.
[3] C. C. Harris, K. L. Greer, R. J. Jaszczak, C. E. Floyd, E. C. Fearnow, and R. E. Coleman, "Tc-99*m* attenuation coefficients in water-filled phantoms determined with gamma cameras," Med. Phys., vol. 1, pp. 681-685, 1984.
[4] I. S. Sayed, "Use of a Tin (Sn) Flat Sheet as a Material Filter for Reduction of Scattered Gamma Photons and Enhancement of Cold Regions Image Quality in Tc-99m SPECT," International Journal of Computing Academic Research (IJCAR)., vol. 5, pp.110-121, 2016.
[5] M. Pillay, B. Shaprio, and P. H. Cox, "The effect of an alloy filter on gamma camera images," Eur. J. Nucl. Medicine., vol. 12, pp. 293-295, 1986.
[6] K. K. Pollard, A. N. Bice, J. F. Eary, L. D. Durack, and T. K. Lewellen, "A method for imaging therapeutic doses of Iodine-131 with a clinical gamma camera," J Nucl. Med., vol. 33, pp. 771-777, 1992.
[7] T. J. Spinks and S. I. Shah, "Effect of lead filters on the performance of a Neuro-PET tomograph operated without septa," IEEE Trans. Nucl. Sci. vol. 40, pp. 1087-1091, 1993.
[8] I. S. Sayed and A. A. Shah, "Modified PET/SPECT Cylindrical Phantom. Proc. IFMBE World Congress on Medical Physics and Biomedical Engineering," Springer-Verlag., vol. 4, pp. 1681-1683, 2007.
[9] A. A. Shah, "Standard Energy Window Data Correction for Scattered Gamma Photons in Single Photon Emission Computed Tomography (SPECT)," Thesis, University of Sindh, Jamshoro, Pakistan, 2007.
[10] W. S. Rasband, "ImageJ," U. S. National Institutes of Health, Bethesda, Maryland, USA, 1997-2015. http://imagej.nih.gov/ij